Egyptian Journal of Cell and Tissue Research
Print ISSN: 2812-5436 / Online ISSN: 2812-5444

Histological Evaluation of the Effect of Lactoferrin on Experimentally Induced Liver Fibrosis in Adult Male Albino Rat

Shimaa Mahmoud Badr [1], Hoda Ali Mohammed Ibrahim [2], Maram Mohamed Elkelany[1]

[1] *Lecturer of Histology and Cell Biology Department, Faculty of Medicine, Tanta University, Tanta, 31527, Egypt.*

[2] *Lecturer of Medical Biochemistry and Molecular Biology*

Abstract

Background: Carbon tetrachloride (CCl4)-induced liver fibrosis is a well-established model of hepatotoxicity. Lactoferrin (LF) is an iron-binding glycoprotein that has anti-inflammatory and antioxidant effects. **Aim of the study:** This study was made to demonstrate the ameliorating effect of lactoferrin versus CCL4 induced liver fibrosis in adult male albino rat using various biochemical and histological techniques. **Materials & Methods:** This study involved forty adult male albino rats that were randomly divided into 4 groups: group I represented the control group, group II received LF (100mg/kg/day) orally for 5 weeks**,** group III was intraperitoneally injected with CCL4 (1ml/kg/once a week, for five weeks) for induction of liver fibrosis, and group IV received LF and CCL4 concomitantly in the same dose and manner as groups II & III respectively. The liver specimens were processed for different biochemical, histological and immunohistochemical techniques. Morphometrical and statistical studies were also performed. **Results:** CCL4 group showed disorganization of liver architecture that was evidenced by light & electron microscopic examination. A significant increase of the mean area percentage of collagen fibers by Masson's Trichrome, immunopositive reaction of αSMA and CD133 along the sinusoids were also observed. Lactoferrin administration in group IV showed improvement of all the previous results and oxidative stress biomarkers. **Conclusion:** Liver fibrosis could be ameliorated by lactoferrin.

Running title: Lactoferrin can suppress liver fibrosis.

Keywords: Lactoferrin, liver, CCL4, ultrastructure, CD133, α-SMA.

1. Introduction

The liver is always susceptible to various harmful chemicals due to its site in the human body. Currently, many individuals suffer from liver diseases induced by several agents as alcohol, chemicals like carbon tetrachloride (CCl4) and paracetamol.[1]

The most common pathological consequence for the majority of chronic liver injuries is hepatic fibrosis. Cirrhosis is the last stage of it which is irreversible, a leading cause of morbidity and mortality globally and has no effective treatment. It is characterized by massive fibrous scarring.[2] Chronic liver injury induced by CCl4 in rats develops liver fibrosis with biochemical and histological models resembling liver cirrhosis in human.[3]

Carbon tetrachloride (CCl4) is a xenobiotic that is used in research to induce liver damage. It is colorless, transparent, volatile liquid.[4,5] It was historically frequently utilized in cleaning agents, refrigerant precursors, and fire extinguishers. The primary routes that humans could be exposed to CCL4 are by ingestion, cutaneous contact, and inhalation. In addition, low concentrations of CCL4 may be inhaled by the general population through the air. Because of its destructive effects, its uses are now banned, and it is only used in some industrial uses.[6]

Lactoferrin (LF) is an iron-binding glycoprotein found in all exocrine secretions; as sweat, tears, saliva, and is particularly plentiful in milk.[7] LF acts as the first-line defense against bacterial, viral, and fungal infections. Moreover, it has anti-inflammatory, anticancer and antioxidant effects. Additionally, it promotes wound healing and bone development.[8]

The effects of hepatoprotective medications with potential therapeutic benefits for usage in humans can be studied using the rat model of liver fibrosis. Therefore, we aimed in this research to evaluate the ability of LF to stop the development and progression of CCl4-induced liver fibrosis in rats by different biochemical and histological techniques.

2. Materials and Methods:

Experimental Animals

Forty adult male albino rats aged 3 months with average weight 200 g were involved in this experiment. The experimental animals were exposed to suitable laboratory conditions and were left for a week to adapt to their new environment before starting the experiment. The experimental design and handling procedures were performed consistent with the guideline of the Ethical Committee of Tanta University (Approval number: 36264PR48/1/23).

Chemical Reagents

- Carbon tetrachloride (CCL4) was obtained in the form of liquid (concentration 100%) from El-Gomhoria Company for Trading Pharmaceutical Chemicals and Medical Appliances, Tanta, Egypt. CCL4 was mixed with olive oil (1:1 ratio).

- Lactoferrin (LF) was purchased from EIPICO Pharmaceuticals, (No.:1200/2021, 10th of Ramadan City, Egypt) in a powder form that was dissolved in distilled water.

Induction of liver fibrosis

Liver fibrosis was induced by intraperitoneal injection with CCl4 at the dose of 1ml/kg body weight once a week for five weeks.[9]

Study design

The rats were divided into four groups (each group included10 rats) as following:

- *Group I:* represented the control group that were divided into 3 subgroups:

Subgroup (i)*:* 4 rats kept without any treatment until the end of the experiment.

Subgroup (ii): 3 rats, each one received 0.5 ml of distilled water (the diluting vehicle for LF) once orally daily for 5 weeks.

Subgroup (iii): 3 rats, each one was intraperitoneally injected by 0.2 ml of olive oil (the diluting vehicle for CCL4) once a week, for five weeks.

- *Group II (LF-group):* each rat received LF at the dose of (100mg/kg/day once orally daily for 5 weeks).[10]
- *Group III (CCL4-group):* rats were used as a model for induction of liver fibrosis as described above.[9]
- *Group IV (LF+CCL4- group):* rats received LF and CCL4 concomitantly in the same dose and manner as groups II & III respectively.

Blood and tissue sampling

Finally, all animals were anaesthetized with 50 mg/kg intraperitoneal injection of sodium pentobarbital.[11] Blood samples were obtained and collected in sterile tubes, then it were centrifuged for 20 minutes. Serum samples were gathered and frozen at −20°C for further biochemical analysis. The liver was excised, part of it was washed with ice cold saline and allowed to dry by filter paper. Then it was homogenized as 10% (w/v) in cold 50 mM phosphate buffer (pH 7.4). It was then centrifuged by a Potter–Elvenhjem tissue at 5000×g at 4 °C for 20 min. The resulting supernatant was parted into aliquots and stored at −80 °C till biochemical analysis.

Biochemical analysis

1. Measurement of serum liver biomarkers: Serum level of alanine aminotransferase (ALT), aspartate aminotransferase (AST), alkaline phosphatase (ALP), total protein, albumin and serum bilirubin were measured

by colorimetric method using available commercial kits bought from (Biodiagnostic company, Giza, Egypt) Catalog No. AL 1031, AS 1061, AP 1020, TP 2020, AB 1010 and BR 1111 respectively.

2. Measurement of malondialdehyde (MDA) and reduced glutathione (GSH) in liver tissue homogenate.

MDA and GSH levels were measured in liver homogenate by colorimetric method using available commercial kits provided by (Biodiagnostic Company, Giza, Egypt) Catalog No.MD 2529 and GR 2511 respectively. All the biochemical analysis were performed using spectrophotometer (BTS-350) in Biochemistry Department, Faculty of Medicine, Tanta University.

Processing for light microscopy:

A midline incision in the anterior abdominal wall was done to dissect and excise the liver. The right lobe of liver was cut into three parts; one part was processed for light microscopic study, one for electron microscopic study and the last one used for biochemical analysis as discussed before. All these steps were performed in the Histology and Cell Biology department, Faculty of Medicine, Tanta University.

Specimens were immediately fixed in 10% formal saline solution for one day, dehydrated in ascending concentrations of ethyl alcohol, cleared in xylene, impregnated and paraffinized. Next, paraffin sections (5 µm thickness) were cut and mounted on slides. Then, sections were stained with hematoxylin & eosin (H&E) and Masson's trichrome stains. [12]

5-µm-thick sections were used for immunohistochemical staining for detection of CD-133 and α-smooth muscle actin (α-SMA). Antigen retrieval of deparaffinized sections was done by adding citrate buffer (pH 6.0) in the microwave. Then deactivation of endogenous peroxidase was performed by incubation in 3% hydrogen peroxide followed by washing with PBS. After that, incubation of the slides with diluted (1:100) primary antibody: Rabbit anti-rat polyclonal for CD-133 (Cat. No.PA5-38014 obtained from Invitrogen, Carlsbad, United States), Mouse anti-rat monoclonal for α-SMA (Cat. No. Mob001 obtained from Diagnostic Biosystems, United States). The sections were then immersed in PBS and incubated with secondary antibodies for 30 min at room temperature: Goat anti-rabbit for CD-133, goat anti- mouse immunoglobulins for α-SMA.

Incubation of the sections with diaminobenzidine (DAB) was done for visualization of antibody binding, and tissue sections were counter-stained with hematoxylin. Negative control was performed by the similar preceding steps without adding the primary antibody. Positive control was: Jurkat cell lysate for

CD-133, Colon and leiomyoma for α-SMA. The positive immunoreactivity appeared as cytoplasmic brown particles or patches.[13, 14,15]

A light microscope (Olympus, Japan) with a built-in camera was used to examine and photograph the slides in the Histology and Cell Biology department, Faculty of Medicine, Tanta University.

Histological scoring was performed according to Modified Metavir [16] using the following criteria: F 0: no fibrosis (normal), F1: fibrosis of portal areas± short fibrous septa, F2: fibrosis of most portal areas with occasional portal to portal (P-P) bridging, F3: fibrosis of most portal areas with obvious portal to portal (P-P) bridging as well as portal to central (P-C), F4: cirrhosis.

Processing for electron microscopy:

Liver specimens were finely cut and fixed using 4% phosphate-buffered glutaraldehyde (0.1 mol/L, pH 7.4), then post-fixed using 1% osmium tetroxide. Subsequently, specimens were dehydrated in ascending grades of alcohol. Then, sections were immersed in propylene oxide then were embedded in epoxy resin mixture. Semithin and ultrathin sections were cut using ultramicrotome. Ultrathin sections were double stained with uranyl acetate and lead citrate [17] to be examined and photographed by JEOL-JEM-100 transmission electron microscope (Tokyo, Japan) at the Electron Microscopy Unit, Tanta Faculty of Medicine, Egypt.

Morphometric study:

For morphometric analysis, the software "ImageJ" (version 1.48v National Institute of Health, Bethesda, Maryland, USA) was used. Non-overlapping 10 fields for each slide in each group were examined at a magnification of 100x and 400x to quantitatively evaluate the histological scoring in Masson's trichrome stained slides [16] and the mean area% [18] in the followings:

1- Collagen fibers in Masson's trichrome stained slides.

2- CD133-immunostained slides (to detect hepatic stellate cells). [19]

3- α-SMA -immunostained slides (to detect transdifferentiation of hepatic stellate cells to myofibroblasts). [20]

Statistical analysis:

The morphometric results were analyzed using one-way analysis of variance (ANOVA) followed by the Tukey post hoc test. Data were displayed as means ± standard deviation (SD). Differences were interpreted as statistically significant if the probability value $p < 0.05$ and extremely significant if $p < 0.001$, while $p > 0.05$ was considered statistically insignificant.[21]

3. Results:

In the present work, no mortality was recorded during the experimental period.

The histological, immunohistochemical and electron microscopic results revealed similar findings in the three subgroups of the control group I (i, ii, iii) with no significant differences in the morphometric results in-between them. Also, biochemical results showed non-significant statistical difference in-between these subgroups. Therefore, they were denoted as control group (I) in text, tables, and figures to simplify our results. As regards group II (LF-group) it also showed no difference in the biochemical, histological results or statistical analysis when compared with control group.

Biochemical results:

1-Effect of lactoferrin on serum liver biomarkers

Serum liver biomarkers levels were increased in CCL4 treated group in comparison to other groups ($P<0.001$). Lactoferrin co-treatment significantly decreased liver biomarkers levels ($P<0.001$) as compared to CCL4 treated group **(Table 1).**

2- Effect of lactoferrin on liver tissue homogenate MDA and GSH levels

Oxidative stress biomarker, malondialdehyde (MDA) level showed an extreme significant increase in liver tissue homogenate in CCL4-treated group compared to other groups ($P< 0.001$). On the other hand, lactoferrin co-treatment significantly decreased the preceding oxidative stress biomarker ($P< 0.001$) as compared to CCL4 treated group (Histogram.1).

The antioxidant biomarker, reduced glutathione (GSH) showed an extreme significant decrease in CCL4- treated group when compared to other studied groups ($P< 0.001$). On the other hand, lactoferrin co-treatment significantly increased GSH level in liver tissue homogenate ($P < 0.001$) as compared to CCL4 treated group (Histogram.2).

Light microscopic results

1-H&E results

Examination of slides from the control group (group I) depicted the histological structure of liver parenchyma composed of ill-defined hexagonal classic lobules. Each lobule was formed of branching and anastomosing cords of hepatocytes radiating from the central vein and separated by blood sinusoids. At the angles of the lobules, portal areas contained branches of the hepatic artery, portal vein and bile ducts were present. Hepatocytes appeared with eosinophilic cytoplasm, pale nuclei with prominent nucleoli. Kupffer cells and endothelial cells were present lining the blood sinusoids **(Figure 1-A&B).**

In CCL4- group (group III), most hepatocytes depicted vacuolated cytoplasm

while other cells appeared with fading nuclei or even anucleated. Dilated congested central veins and portal vein branches with severe mononuclear cellular infiltration were evident. The portal area showed proliferated dilated bile ductules lined by cholangiocyte. Dilated blood vessel lined by partially desquamated endothelium with subendothelial and medial vacuolations was evident within the portal area. Kupffer cells were distributed within the blood sinusoids which appeared congested **(Figure 1- C,D,E,F&G).**

LF+CCL4 group (group IV) examination exhibited marked improvement in congestion & cellular infiltration within the central vein and portal areas. Most of hepatocytes depicted decrease in the vacuolations and appeared with acidophilic cytoplasm with rounded vesicular nuclei & prominent nucleoli (**Figure 1-H&I**).

2-Masson's *trichrome stained sections results*

Examination of control group sections revealed few collagen fibers were detected encircling the central vein and in the portal areas **(Figure 2-A)**. In CCL4-group (group III), collagen fibers significantly increased as compared to that in control group; numerous collagen fibers appeared around the central veins and in the portal areas with formation of fibrous septa reached neighboring portal areas **(Figure 2-B)**. In LF+CCL4 group (group IV), collagen fibers significantly decreased as compared to that in CCL4-group; few collagen fibers appeared around the central veins and some collagen fibers in the portal areas **(Figure 2-C)**.

3-α-SMA immunohistochemical results

The control group (group I) exhibited brownish cytoplasmic immunostaining for α-SMA in the cytoplasm of the smooth muscles of the vessels wall of central veins and in branches of portal veins & hepatic arteries **(Figure 2-D)**. CCL4-group (group III) showed widespread strong brownish cytoplasmic immunostaining for α-SMA along the blood sinusoids and the cytoplasm of smooth muscles of vessels wall within the portal area and central veins **(Figure 2-E)**. Concerning LF+CCL4 group (group IV), it displayed limited positive cytoplasmic immunostaining in the smooth muscles of the wall of central vein as well as the portal vessels and weak reaction along the blood sinusoids **(Figure 2-F)**.

4-CD133 immunohistochemical results:

The control group showed moderate CD133 immunohistochemical staining in the cytoplasm of cells along sinusoids and negative reaction in vessel wall **(Figure 2-G)**. However, CCL4-group (group III) revealed strong CD133 immunostaining in

the cytoplasm of numerous cells along the sinusoids **(Figure 2-H)**. Contrary, LF+CCL4 group (group IV) exhibited results identical to control group **(Figure 2-I)**.

Morphometric and statistical analysis results:

Statistical analysis of the mean area percentage of collagen fibers, α SMA and CD133 of CCL4-group (group III) exhibited extremely significant increase ($P<0.001$) in the three parameters (34.221±14.29, 13.421±4.35, 18.157±4.09 respectively) as compared to control group (12.568±5.64, 2.759±2.05, 6.859±4.52 respectively). LF+CCL4 group (group IV) showed non-significant statistical difference ($P>0.05$) in the mean area percentage of collagen (19.306±5.33) as compared to control group but, it showed significant increase in the mean area percentage of α SMA and CD133 (7.267±3.62, 14.966±6.23 respectively) as compared to control group. Statistical analysis of histological scoring of group III showed extremely significant increase compared with control group ($P<0.001$). While group IV showed nonsignificant difference($P>0.05$) with control group **(Histogram. 3).**

Electron microscopic results

Examination of liver sections from the control group (group I) by transmission electron microscopic (TEM) depicted hepatocytes which were polygonal in shape, with central rounded euchromatic nuclei. The cytoplasm was rich in mitochondria and rough endoplasmic reticulum. Between adjacent hepatocytes, bile canaliculi were present. Within the perisinusoidal region, star shaped hepatic stellate cell was detected. The cytoplasm of hepatic stellate cell confined heterogenous electron dense lipid droplets; its nucleus was indented by lipid droplets **(Figure 3-A&B).**

Examination of ultrathin sections of CCL4-group (group III) revealed hepatocytes with rarified cytoplasm, dilated rER, mitochondria with disrupted cristae, irregular nuclear membrane and shrunken irregular nuclei with clumped chromatin. Kupffer cell with large, kidney shaped nucleus could be detected. Hepatic stellate cell appeared with few lipid droplets and surrounded by cross sections of collagen bundles **(Figure 4-A,B,C,D,E&F)**.

Regarding LF+CCL4 group (group IV), hepatocytes appeared with euchromatic nuclei. Rough endoplasmic reticulum, mitochondria, and rarified areas within the cytoplasm were present. Hepatic stellate cell appeared with heterogenous electron dense few lipid droplets **(Figure 5-A&B).**

Table (1): Serum liver biomarkers among the studied groups.

	Group I	**Group II**	**Group III**	**Group IV**
ALT (unit/ml)	35.8 ± 3.9	35.9 ± 4.2	115.4 ± 8.5***	37.8000±2.4
AST (unit/ml)	25.2 ± 2.7	24.6 ± 3.9	91.1 + 5.1***	27.8± 3.01
ALP (IU /L)	174.5 + 12.3	173 + 13.9	468.2 ± 39.8***	184.0000± 6.4
Total protein (gm/dl)	7.96 ± 0.52	7.75 ± 0.53	2.91 ± 0.51***	7.6200± 0.26
Albumin (gm/dl)	4.85 ± 0.57	4.88 + 0.46	1.56 ± 0.48***	4.9400± 0.38
Total bilirubin (mg / dl)	0.76 ± 0.13	0.77 + 0.12	3.6500± 1.6***	0.7740± 0.17

Abbreviations: Alanine aminotransferase (ALT), Aspartate aminotransferase (AST), Alkaline phosphatase (ALP).

Data are expressed as mean ±standard deviation. ***P <0.001 is extremely significant value versus control group

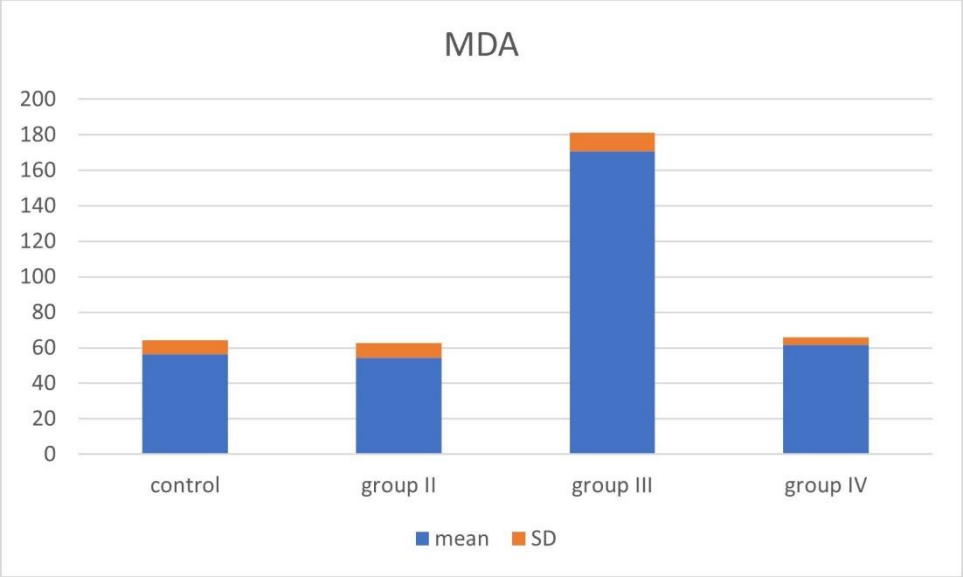

Histogram (1): Effect of lactoferrin treatment on oxidative stress biomarker; MDA level in liver tissue homogenate in control and experimental groups.

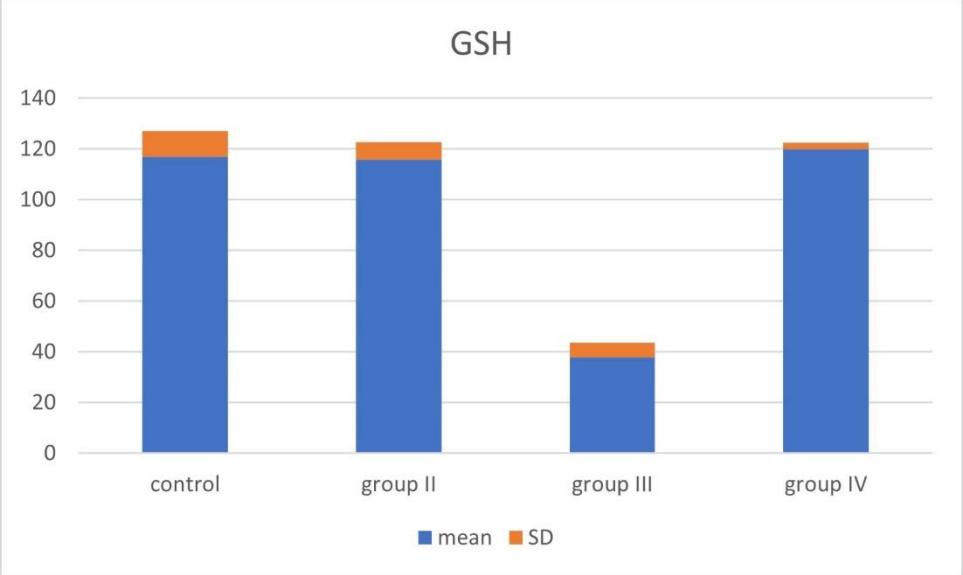

Histogram (2): Effect of lactoferrin treatment on oxidative stress biomarker; GSH level in liver tissue homogenate in control and experimental groups.

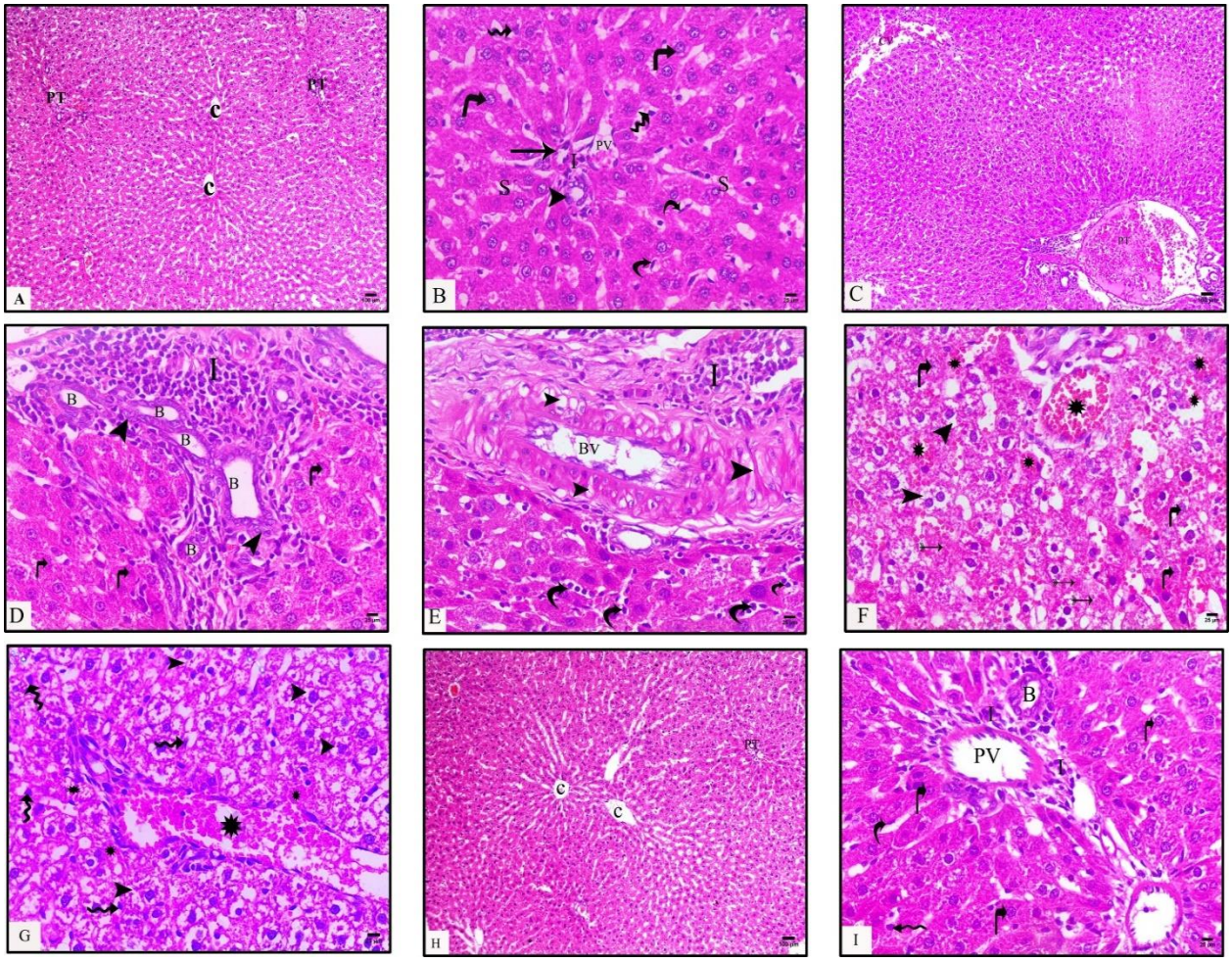

Fig. 1: Photomicrographs of the liver tissue from the studied groups: control **(A&B)** showing: normal architecture of the liver with ill-defined classic hepatic lobules. Central veins (C) are present in the center of the lobules, and portal tracts (PT) are noticed at the periphery of the lobules. Hepatocytes are arranged in anastomosing cords and displaying acidophilic cytoplasm and central rounded vesicular nuclei with prominent nucleoli (angled arrows). Hepatocytes cords are separated by blood sinusoids (S) that are lined by endothelial cells with flat nuclei (curved arrows). Kupffer cell nuclei are noticed (wavy arrows). Portal tracts are formed of portal vein branch (PV), hepatic artery branch (arrow) and bile ductules (arrow head). A few mononuclear cells are also present (I). CCL4-group **(C,D,E,F&G)** show disturbed liver architecture with dilatation, congestion in central vein (cv) and within the portal area (PT). D&E shows proliferated bile ductules lined by cholangiocyte (B). Dilated blood vessel (BV) with partially desquamated endothelium with subendothelial and medial vacuolations (arrow heads) and surrounded by perivascular mononuclear cellular infiltration extending into both portal area (I) and in sinusoids (curved arrows). Some hepatocytes appear with fading nuclei (angled arrows). **F&G** show either vacuolated hepatocytes (arrow heads) or anucleated one

(feathery arrows) or with fading nuclei (angled arrows). Moreover, dilated congested both blood sinusoids and portal vein branch (stars) and many Kupffer cell nuclei are also present (wavy arrows). LF+CCL4 group (H&I) show central veins (c) with radially arranged hepatocytes and more or less normal portal area (PT) formed of portal vein branch (PV), bile ductule (B) and mononuclear cells (I). Most hepatocytes have acidophilic cytoplasm and rounded nuclei with prominent nucleoli (angled arrows) separated by blood sinusoids lined by flat endothelial cells (curved arrow) and Kupffer cell nuclei (wavy arrow) also appear. (H&E, Mic.Mag. A,C&H x100 scale bar =100 µm, B,D,E,F,G&I x400 scale bar =25 µm).

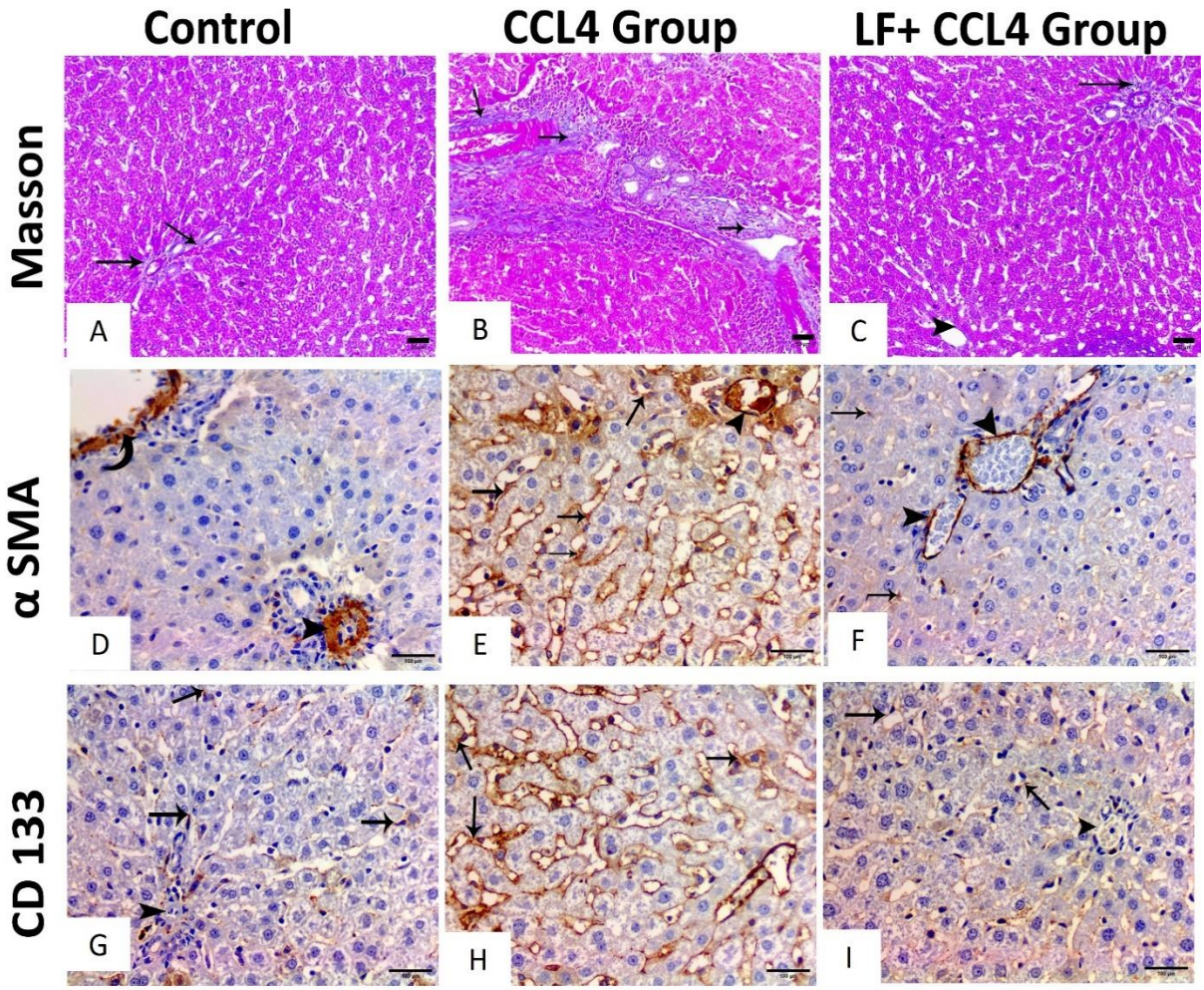

Fig. 2: Photomicrographs of Masson's trichrome-stained, α-SMA and CD133-immunostained liver sections of the studied groups. (A) Control group shows blue stained thin strands of collagen fibers around portal area (arrows). (B) CCL4-group shows wide spread of thick blue stained collagen bundles at the portal areas (arrows). (C) LF+CCL4- group shows thin blue stained collagen fibers localized around central vein (arrow head) and portal area (arrow).

(Masson's trichrome, Mic. Mag. x200, scale bar =50 µm). (D) Control group: shows positive cytoplasmic immunostaining in the smooth muscles of the walls of both the central vein (curved arrow) and a vessel wall in the portal area (arrow head). (E) CCL4-group: shows strong positive cytoplasmic immunostaining along the sinusoids (arrows) and the cytoplasm of smooth muscles of vessels wall (arrow heads). (F) LF+CCL4- group: shows weak positive cytoplasmic immunostaining along the sinusoids (arrows) and strong positive cytoplasmic immunoreaction in the smooth muscles of vessel wall (arrow head). (α-SMA immunostaining, Mic. Mag. x400, scale bar =100 µm). (G) Control group: shows moderate CD133 positive immunostaining in few cells along the sinusoids (arrows) and negative reaction in vessel wall (arrow heads). (H) CCL4-group: shows strong CD133 positive immunostaining in numerous cells (arrows) along the sinusoids. (I) LF+CCL4- group: showing results identical to control group (CD133 immunostaining, Mic. Mag. x400, scale bar =100 µm).

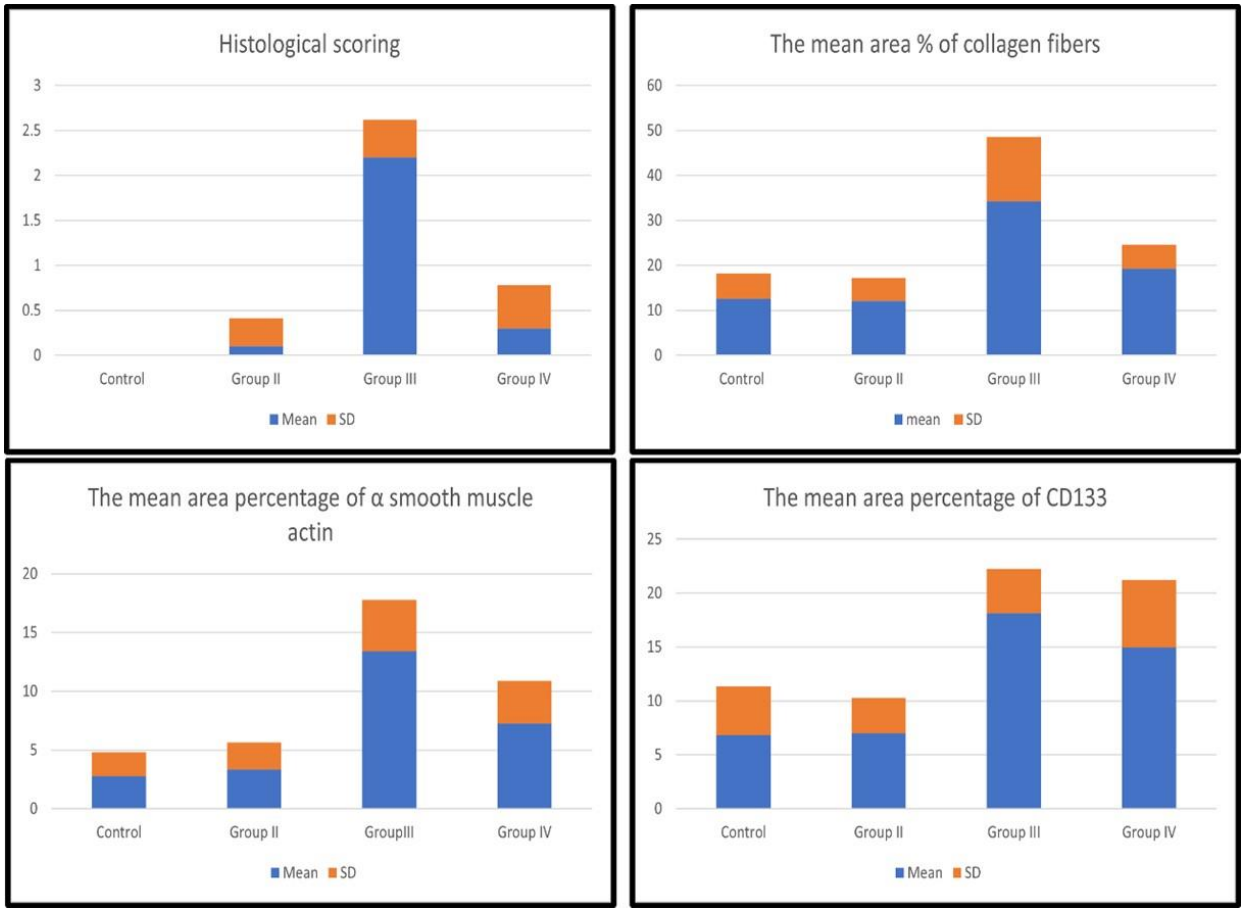

Histogram. 3: Morphometrical and statistical analysis of light microscopic results: (a) Histological scoring (b) Mean area % of collagen fibers (c) Mean area percentage of αSMA (d) Mean area percentage of CD133.

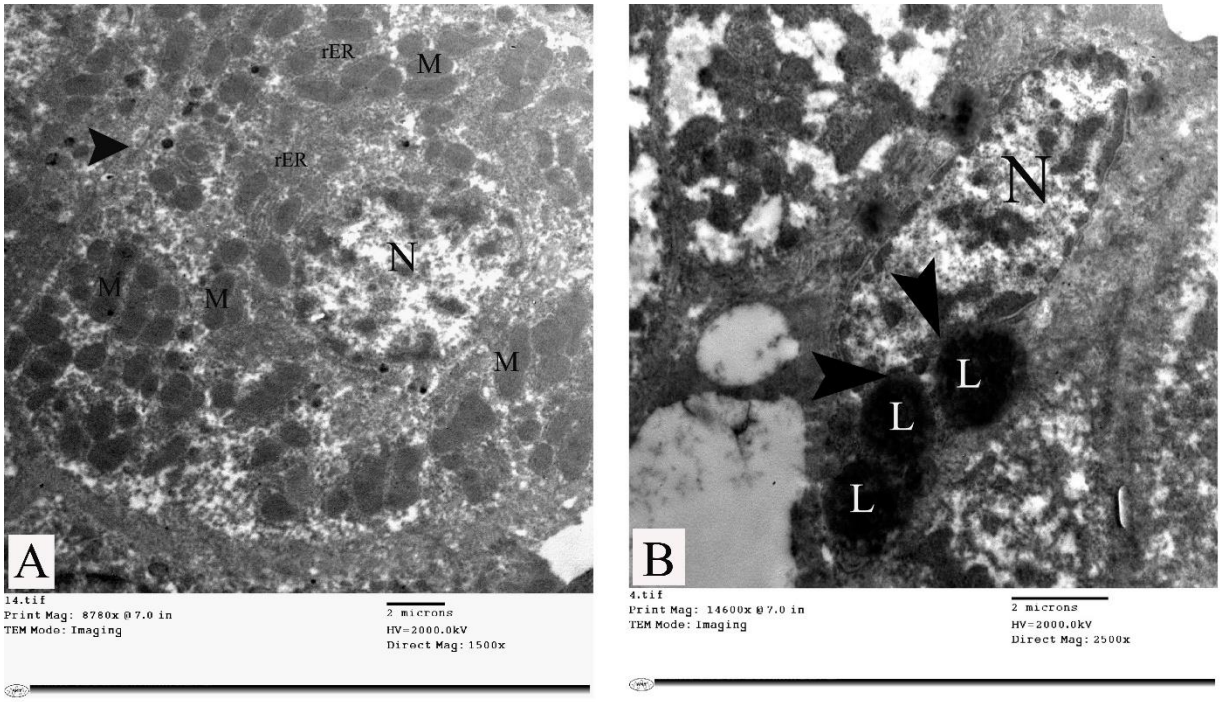

Fig.3: An electron micrograph of liver ultrathin sections of control group (group I): (A) shows hepatocyte with euchromatic nucleus (N), multiple mitochondria (M), dispersed rough endoplasmic reticulum (rER). Bile canaliculus (arrow head) appears in between hepatocytes. (B) shows hepatic stellate cell within the perisinusoidal space with its euchromatic nucleus (N) which is indented (arrow heads) by lipid droplets (L). (Mic. Mag. A x 1500, B x 2500).

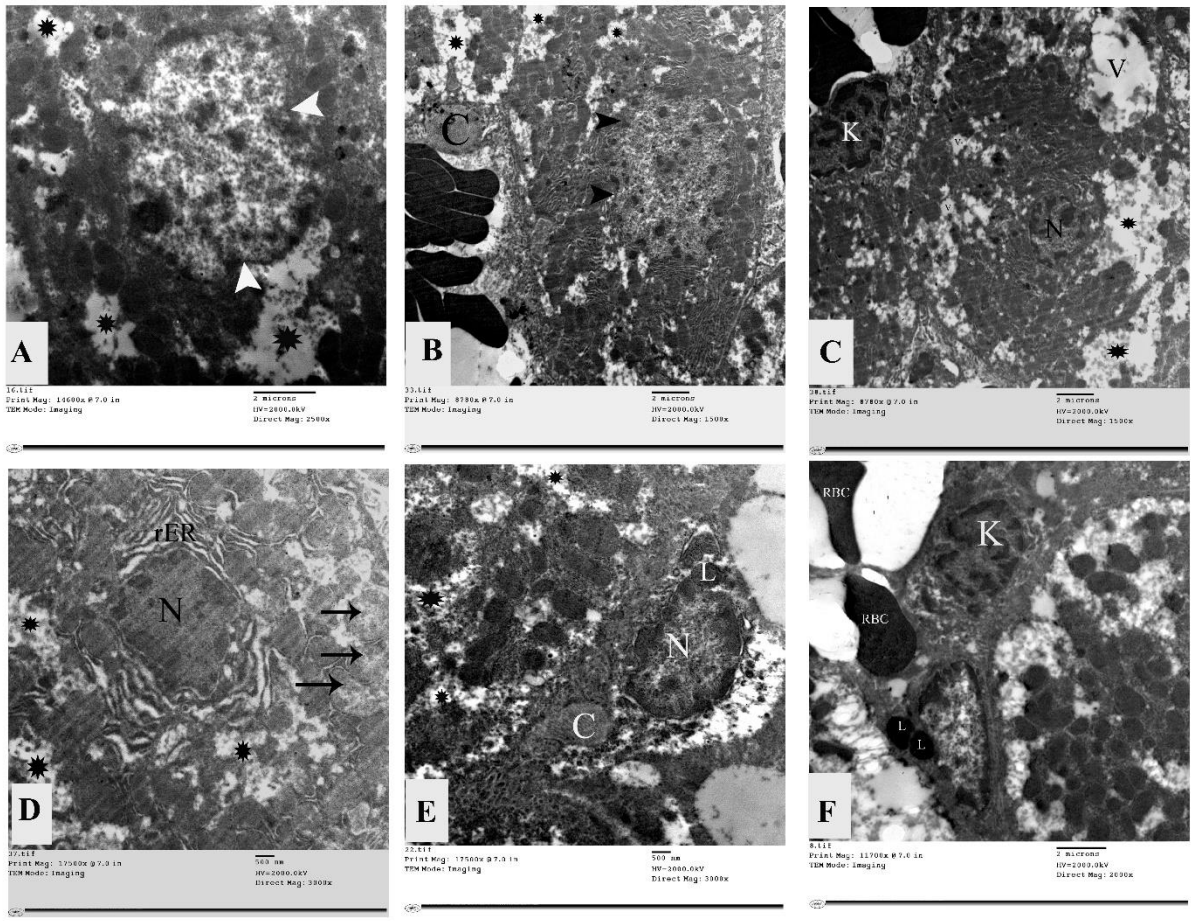

Fig. 4: An electron micrograph of liver ultrathin sections of CCL4 group (group III) show some hepatocytes with irregular nuclear membrane (arrow heads) and others show shrunken irregular nuclei (N) with abnormal clumped chromatin as in D. Moreover, the cytoplasm shows prominent dilated rER (rER), swollen mitochondria with disrupted cristae (arrows), vacuolation (V), and rarefaction (stars). Kupffer cell nucleus (K) with its characteristic kidney shape appearance is observed, and collagen bundles (C) appear. Notice presence of hepatic stellate cell -between hepatocyte and sinusoid containing (RBCs)- with nucleus (N) indented by lipid droplets (L). (Mic. Mag. A x 2500, B&C x 1500, D x 3000 E x 3000 & F x 2000).

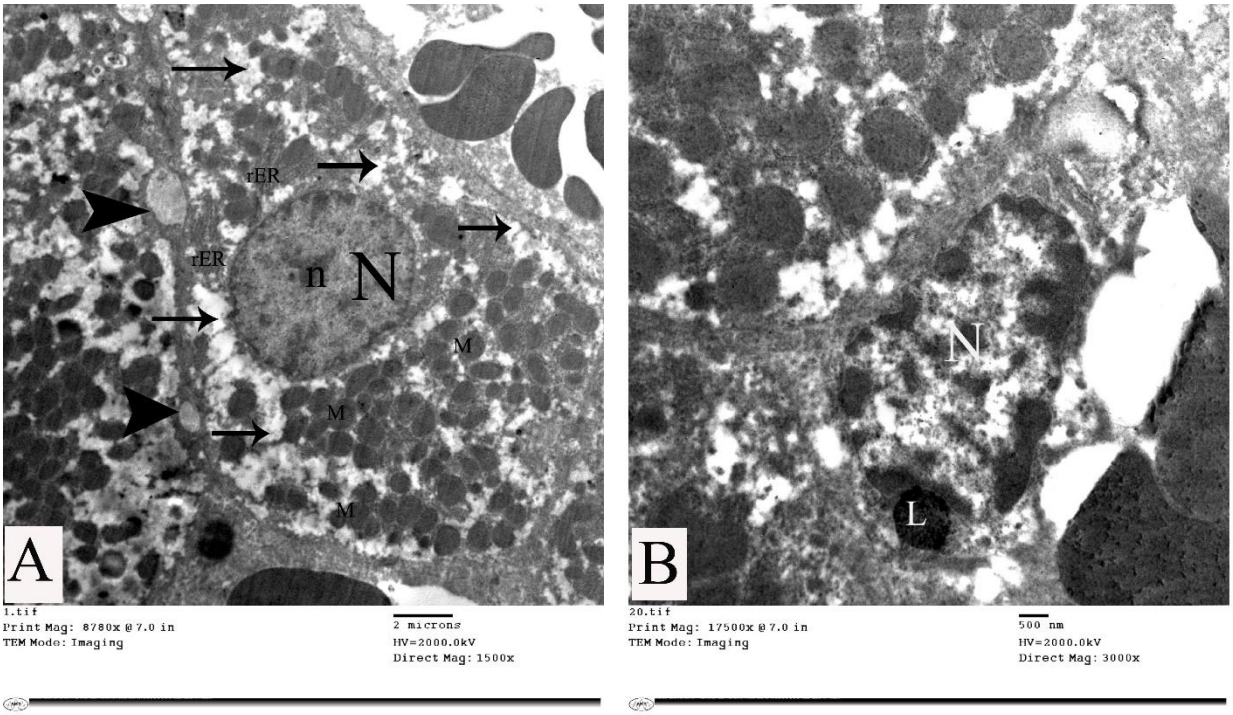

Fig. 5: An electron micrograph of liver ultrathin sections of LF+CCL4- group (group IV): (A) shows hepatocyte with rounded euchromatic nucleus (N) and prominent nucleolus (n), mitochondria (M), rER (rER) and areas of rarified cytoplasm (arrows). Bile canaliculi (arrow heads) are also noticed. (B) shows part of hepatocyte surrounded by hepatic stellate cell with its nucleus (N) indented by single lipid droplet (L) (Mic. Mag. A X1500, B X3000).

4. Discussion:

CCl4-induced liver fibrosis is a well-established model of hepatotoxicity.[22] Previous study by **Aoyama et al.**[7] observed that LF improved liver fibrosis in steatohepatitis model. Therefore, the current study aimed to demonstrate the therapeutic effect of lactoferrin on CCl4 induced liver fibrosis in rats.

Guang and Yun [23] attributed the liver injury induced by CCL4 to stimulation of endogenous reactive oxygen. Previous studies reported that LF may decrease oxidative stress. The binding affinity of LF to the cells limits the process of membrane lipid peroxidation, as LF is not fully saturated and can scavenge free iron radicals.[24] Moreover, **SH et al.** [25] stated that increased MDA level is a main sign of endogenous lipid peroxidation. This goes in line with the current study, as LF decreased the MDA levels in liver tissue of rats.

The current work showed alterations in serum liver biomarkers in CCL4- treated group, this goes in line with **Frank et al.** [26] who stated that

CCl4 causes loss of hepatic parenchyma and subsequent dysregulation of the liver's metabolic and synthetic functions. Moreover, they added that changes of serum enzyme activity levels denote injury to hepatocytes or cholangiocytes.

Unfortunately, it is not widely known how liver fibrogenesis actually occurs. It is believed that myofibroblasts and hepatic stellate cells (HSCs) are essential in the development of liver fibrosis, which includes the substantial remodeling of extracellular matrix (ECM) elements and the deposition of collagen type I and III. The activated HSCs/myofibroblasts, particularly the transitional form of HSCs (T-HSCs), are the chief fibrogenic cell type in the liver, and constitute a main source of fibril-forming ECM.[27] The aim of anti-fibrotic therapy is thought to be the imbalance between the synthesis and breakdown of ECM by HSC, which has been identified as a key factor in the fibrogenesis of liver fibrosis. Moreover, the myofibroblast acts as a primary cellular mediator of fibrosis as it is the main collagen-producing cell.[22]

In this result, inflammatory cells infiltration was noticeable and identical to the findings of **Cosgun et al.**[5] during studying CCL4-induced liver fibrosis and **Emam et al.**[28] who studied thioacetamide induced hepatotoxicity. **Omara et al.**[29] **& Elufioye and Habtemariamb** [30] related it to both local and systemic inflammation, which is a hallmark of drug-induced liver damage. As a result, macrophages and neutrophils are attracted into the liver's blood vessels to clear away debris and dead cells in order to promote tissue regeneration.

Previous study by **Farid et al.** [31] observed that when LF was administered for defense against CCl4, it caused inactivation of monocytes and macrophages as manifested by a significant decrease of both pro- and anti-inflammatory mediators. Moreover, other studies [25,10] stated that LF has anti-inflammatory activity, as it can control cytokine manufacture by macrophages and lymphocytes. LF can also reduce inflammation by preventing iron-catalyzed free radical damage at inflammatory sites. Additionally, previous study by **Tanaka et al.**[32] indicated that LF inhibited inflammation in a dextran sulfate sodium-induced colitis model in rats and mice.

Dilated congested central veins, blood sinusoids, and portal veins were observed in CCl4- treated group. This goes in line with **Venkatanarayana et al.**[33], **Abu-Dief et al.**[18] **&Naz et al.**[34] who observed similar findings in their studies on CCl4 induced liver injury. It may be attributed to increased prostaglandin synthesis as documented by **Hassan et al.**[35] who stated that prostaglandin causes

smooth muscle relaxation and dilation of blood vessels. Also, they added that congestion may be caused by loss of fluid from dilated vessels, so the vessels appeared to be filled with RBCs. On the other hand**, Abdeen et al.**[36] explained vascular dilatation to the stimulation of Kupffer cells with consequent increase in the synthesis of nitric oxide which acts as a vasodilator.

Proliferation and branching of bile ductules within the portal area were prominent in CCL4 group. This was explained by **Kumar et al.**[37] who stated that, in most cases of liver failure, the liver progenitor cells tend to differentiate into cholangiocytes, that leads to an insufficient increase in parenchymal tissue and greater growth of ductular structures. The origin of stem cells during ductular growth could involve cholangiocytes, hepatocytes, or hepatic progenitor cells.

The CCl4-treated group showed liver fibrosis and excessive deposition of collagen fibers using Masson's trichrome stain and the histological score. The same results were recorded by **Cosgun et al.**[5]**& Ogaly et al.**[38] while studying liver fibrosis induced by CCl4. Moreover, **Moreno et al.**[39]**, Ukairo et al.**[22] **& Abd Elzaher et al.**[40] stated that excessive deposition of collagen and ECM occurs due to increased expression of transforming growth factor (TGF-β). The over expression of TGF-β has been interrelated with the amount of fibrosis in animal models. Additionally, **Abd Elzaher et al.**[40] stated that toxic hepatocytes stimulate Kupffer cells that secrete TGF-β1. Then, TGF-β1 excites HSCs which rise secretion and deposition of (hepatic collagen-α1) leading finally to fibrosis.

In current research, many α-SMA positive cells were noticed in CCl4-treated group. This finding goes in line with **Khedr and Khedr** [41] &**Abu-Dief et al.**[18] during studying CCL4 induced liver fibrosis. They stated that when HSCs are stimulated, they change into myofibroblasts. Also, this may be confirmed by our ultrastructural finding of decreased lipid droplet of HSCs during its transformation into myofibroblasts in CCl4-treated group. These myofibroblasts are responsible for the hypersecretion of collagen during hepatic fibrogenesis. Moreover, previous studies by **Chen et al.**[4] mentioned that activation of HSCs occurs either directly by oxidative stress or through paracrine stimulation by injured hepatocytes.

It was observed that CD133 was intensely up-regulated in CCl4-treated group. **Fujii et al.**[42] recorded the same finding while studying the mouse model of CCL4 induced liver fibrosis and stated that CD133 positive cells correspond to HSCs.

Fading nuclei of hepatocytes and karyolysis observed in current work were

formerly reported by **Lee et al.**[43] who studied CCl4-induced acute liver damage in mice**.** It may be attributed to CCl4 induced hepatic oxidative stress as stated by **Eldesouky et al.**[44] However, **Zowail et al.**[45] ascribed the previous findings to the disruption of calcium (Ca+2) balance, which results in cell death and necrosis. Ca+2 homeostasis is impacted by CCl4 in different ways. Through lipid peroxidation in damaged cell membranes, it can encourage the influx of calcium ions into the cytoplasm; alternatively, it can do this by opening specific membrane calcium channels. Additionally, it prevents calcium ions from leaving the cell via active transport. Overstimulation of calcium-dependent cellular enzymes by calcium ions results in irreversible cell damage and death.

The swollen mitochondria that were noticed in CCL4-treated group may be a sign of hepatocytes apoptosis. **Amer et al.**[46] stated that mitochondria are the chief organelle that controls apoptosis because they are the main site for energy creation. On the other hand**, Abdeen et al.**[36] attributed mitochondrial abnormalities to reduced intra mitochondrial protein synthesis and rise of cytosolic calcium caused by oxidative stress and respiratory chain dysfunction.

Hepatocyte cytoplasmic vacuolations observed in CCL4 treated group were consistent with those of **Hassan et al.**[35] in experimentally induced fatty liver in rat**; Abu-Dief et al.**[18] &**Fathy et al.**[47] in CCl_4-induced hepatic fibrosis in mice and rats respectively. **Hassan et al.**[35] attributed that to cellular hypoxia. They added that cellular hypoxia lowers the function of plasma membrane ATP-dependent sodium pumps, which causes intracellular sodium and potassium efflux to accumulate. Then water enters the cell, causing cell swelling and ER dilatation.

Rarefaction of the cytoplasm detected in current research may be due to proliferation of smooth endoplasmic reticulum and glycogen accumulation; meanwhile, dilatation of rough endoplasmic reticulum cisternae caused by lipid peroxidation or protein retention due to decreased secretory activity. [34]

LF+CCL4 treated group showed significant improvement of the previous findings. The antifibrotic effect of LF may be attributed to the inactivation of HSC as reported by **Aoyama et al.**[7]**. Ahmed et al.**[24] added that LF stops the TGF-β1-induced fibrosis signaling pathway. Furthermore, **Tung et al.**[10] observed that LF decreased the accumulation of collagen proteins and expression of α-SMA using PCR and Western blotting.

The improvement of the previous finding in LF+CCL4 treated group attributed to that LF prevents endoplasmic

reticulum (ER) stress and facilitates the autophagy of injured hepatocytes due to its capacity to scavenge ROS as reported by **Ahmed et al.**[24] They added that the antiviral properties of LF make it effective versus a wide range of viruses, including hepatitis C. Hepatocellular necrosis was prevented by LF, and liver tissue was directly cytoprotected.

Previous studies [7,31&48] observed that LF stopped fibrosis without any side effects. Current research has shown that lactoferrin prevented the progression of liver fibrosis by using different biochemical, histological, immunohistochemical and ultrastructural methods. So, LF is a protective or therapeutic agent for fibrosis.

5. Conclusions:

Based on the above-discussed results, it is concluded that lactoferrin is beneficial in ameliorating the histological structural changes that occurred in CCL4-induced model of liver fibrosis. Accordingly, lactoferrin can be used as an assistant factor during treatment of cases of liver fibrosis.

Conflicts of Interest

The authors assert no conflict of interest.

6. References

1- Bouhrim M, Quassou H, Choukri M, Mekhfi H, Ziyyat A, Legssyer A, et al. Hepatoprotective effect of Opuntia dellenii seed oil on CCL4 induced acute liver damage in rat. *Asian Pac J Trop Biomed.* 2018;8:254-60. doi: 10.4103/2221-1691.233006.

2- Huang YH, Shi MN, Zheng WD, Zhang LJ, Chen ZX, Wang XZ. Therapeutic effect of interleukin-10 on CCl4-induced hepatic fibrosis in rats. *World J Gastroenterol*. 2006;9:1386-1391. doi: 10.3748/wjg.v12.i9.1386.

3- Lee GP, Jeong WI, Jeong DH, Do SH, Kim TH, Jeong KS. Diagnostic evaluation of carbon tetrachloride-induced rat hepatic cirrhosis model. *Anticancer Res.* 2005;25:1029-1038. PMID: 15868943.

4- Chen X, Gao G, Luo W, Wang G, Zheng W, Jia2 Q, et al. Inhibitory effect of Dioscorea panthaica on CCl4-induced liver fibrosis in rats. *Journal of Medicinal Plants Research.* 2012; 6(9):1532-1538. doi: 10.5897/JMPR11.676

5- Cosgun, BE, Erdemli, ME, Gul M, Gul S, Bag GH, Zeynep E, et al. Crocin (active constituent of saffron) improves CCl_4-induced liver damage by modulating oxidative stress in rats. *Turkish Journal of Biochemistry*. 2019; 44:370-378. doi: 10.1515/tjb-2017-0173.

6- El Sayed H, Morsy L, Abo Emara T, Galhom R. Effect of Carbon Tetrachloride (CCL4) on Liver in Adult Albino Rats: Histological study. *The Egyptian Journal of Hospital Medicine.* 2019;76(60):4254-4261. doi: 10.21608/ejhm.2019.43809.

7- Aoyama Y, Naiki-Ito A, Xiaochen K, Komura M, Kato H, Nagayasu Y, et al. Lactoferrin Prevents Hepatic Injury and Fibrosis via the Inhibition of NF-κB Signaling in a Rat Non-Alcoholic Steatohepatitis Model. *Nutrients.* 2021;23;14(1):42. doi: 10.3390/nu14010042. PMID: 35010924; PMCID: PMC8746867.

8- Safaeian L, Zabolian H. Antioxidant effects of bovine lactoferrin on dexamethasone-induced hypertension in rat. *ISRN Pharmacol.* 2014; 22;2014:943523. doi: 10.1155/2014/943523. PMID: 24587916; PMCID: PMC3920649.

9- Singh D, Arya P, Singh V, Arya D, Bhagour K, Gupta R. Role of Cressa Cretica on CCl4- Induced Liver Damage in Experimental Rats. *Journal of Pharmacognosy and Phytochemistry*. 2018; 7(1): 1368-1373.

10- Tung YT, Tang TY, Chen HL, Yang SH, Chong KY, Cheng WT, et al. Lactoferrin protects against chemical-induced rat liver fibrosis by inhibiting stellate cell activation. J Dairy Sci. 2014;97(6):3281-3291. doi: 10.3168/jds.2013-7505. Epub 2014 Apr 14. PMID: 24731632.

11- Ghasi S, Umana I, Ogbonna A, Nwokike M, Ufelle S. Cardioprotective effects of animal grade piperazine citrate on isoproterenol-induced myocardial infarction in Wistar rats: biochemical and histopathological evaluation. *African Journal of Pharmacy and Pharmacology.* 2020; 14(8): 285-293. doi: 10.5897/AJPP.

12- Suvarna S, Layton Ch. Bancroft J. *Bancroft's Theory and Practice of Histological Techniques*. Chapters 10 and 12. 8th ed. China, Elsevier; 2019; 126:166. https://doi. org/10.1016/B978-0-7020-6864-5.01001-X.

13- Yin S, Li J, Hu C, Chen X, Yao M ,Yan M, et al. CD133 positive hepatocellular carcinoma cells possess high capacity for tumorigenicity. *International journal of cancer*. 2007; 120(7):1444-1450. doi: 10.1002/ijc.22476.

14- Buchwalow IB, Böcker W. *Immunohistochemistry: Basics and Methods. Working with Antibodies.* London, Springer Dordrecht Heidelberg; 2010: 31–39. doi: 10.1007/978-3-642-04609-4.

15- Moustafa A. Age-related changes in the immunohistochemical localization pattern of α-smooth muscle actin and vimentin in rat testis. *The Egyptian Journal of Histology.* 2012;35. 412-423. doi: 10.1097/01.EHX.0000418134.14989.85.

16- Nallagangula KS, Nagaraj SK, Venkataswamy L, Chandrappa M. Liver fibrosis: a compilation on the biomarkers status and their significance during disease progression. *Future Sci OA.* 2017;4(1):FSO250. doi: 10.4155/fsoa-

2017-0083. PMID: 29255622; PMCID: PMC5729599.

17- Zaghloul D, Gad-El-Rab WM, Bushra RR, Farahat AA. The possible protective role of methionine against sodium fluoride-induced pancreatic changes in the adult male albino rat: a histological, immunohistochemical and morphometric study. *Egyptian Journal of Histology*. 2019;42(2):285-296. doi: 10.21608/EJH.2019.6198.1040.

18- Abu-Dief E, Mohammed D, Abd El Haliem N, Mohammed S, El-Badry A. Impact of omega-3 fatty acids on evaluation of carbon tetrachloride-(CCL4) induced liver cirrhosis in mice: A histological and immunohistochemical study. *Egyptian Journal of Histology*. 2018;41(1):61-72. doi: 10.21608/EJH.2018.7522.

19- Claus Kordes, Iris Sawitza, Alexis Müller-Marbach, Niloofar Ale-Agha, Verena Keitel, Hanne Klonowski-Stumpe, Dieter Häussinger, CD133+ hepatic stellate cells are progenitor cells. Biochemical and Biophysical Research Communications. 2007; 352(2): 410-417.

20- Carpino G, Morini S, Ginanni Corradini S, Franchitto A, Merli M, Siciliano M, Gentili F, Onetti Muda A, Berloco P, Rossi M, Attili AF, Gaudio E. Alpha-SMA expression in hepatic stellate cells and quantitative analysis of hepatic fibrosis in cirrhosis and in recurrent chronic hepatitis after liver transplantation. Dig Liver Dis. 2005 May;37(5):349-56. doi: 10.1016/j.dld.2004.11.009. PMID: 15843085.

21- Dawson B, Trapp RG. *Basic & Clinical Biostatistics. In: Basic & Clinical Biostatistics*. 4th ed. New York, Lange Medical Books / McGraw-Hill Medical Publishing Division.; 2004:162–189.

22- Ukairo DI, Ojiako OA, Nwaoguikpe R, Ibegbulem CO, Igwe CU, Iheme CI. Ameliorative effects of Nigerian recipes on histopathological and immunohistochemical changes of CCL4-induced hepatic fibrosis in male Wistar rats. *J Pharmacogn Phytochem.* 2017;6(6):1624-1631.

23- Guang HY, Yun HC. Sparassis crispa Attenuates Carbon Tetrachloride-Induced Hepatic Injury in Rats. *Korean J Phys Anthropo.* 2014; 27(3): 113-122. doi.org/10.11637/kjpa.

24- Ahmed KA, Saikat ASM, Moni A, Kakon SAM, Islam R, Uddin J. Lactoferrin: potential functions, pharmacological insights, and therapeutic promises. *J Adv Biotechnol Exp Ther*. 2021;4(2):223-237. doi: 10.5455/jabet.2021.d123.

25- SH A, Alattar HA, Farid AS, Farah KM. Influence of lactoferrin on immune response in rats intoxicated by diazinon. *Benha Veterinary Medical Journal*. 2018;

34(2):169-181. doi: 10.21608/bvmj.2018.29426.

26- Frank D, Savir S, Gruenbaum BF, Melamed I, Grinshpun J, Kuts R, Knyazer B, Zlotnik A, Vinokur M, Boyko M. Inducing Acute Liver Injury in Rats via Carbon Tetrachloride (CCl4) Exposure Through an Orogastric Tube. J Vis Exp. 2020; 28(158):10.3791/60695. doi: 10.3791/60695. PMID: 32420997; PMCID: PMC7859859.

27- Lotowska JM, Sobaniec-Lotowska ME, Lebensztejn DM, Daniluk U, Sobaniec P, Sendrowski K, et al. Ultrastructural Characteristics of Rat Hepatic Oval Cells and Their Intercellular Contacts in the Model of Biliary Fibrosis: New Insights into Experimental Liver Fibrogenesis. *Gastroenterol Res Pract.* 2017;2017:2721547. doi: 10.1155/2017/2721547. Epub 2017 Jul 9. PMID: 28769978; PMCID: PMC5523291.

28- Emam MA, Farouk SM, Abdo M. The ameliorative potential of probiotics and/or silymarin on thioacetamide induced hepatotoxicity in rats: histological and immunohistochemical study. *Int. J. Morphol*. 2018;36(2):661-669. doi: 10.4067/S0717-95022018000200661.

29- Omara E, El-Toumy S, Shabanaa M, Farraga A, Nadac S, Shafeea N. The Antifibrotic Effect of Zilla Spinosa Extracts Targeting Apoptosis in CCl4-Induced Liver Damage in Rats. *Journal of The Arab Society for Medical Research.* 2018; 13:129–143. doi: 10.4103/jasmr.jasmr_29_18.

30- Elufioye T, Habtemariam S. Hepatoprotective Effects of Rosmarinic Acid: Insight into Its Mechanisms of Action. *Biomedicine & Pharmacotherapy*. 2019; 112:108600-108611. doi: 10.1016/j.biopha.2019.108600.

31- Farid AS, El Shemy MA, Nafie E, Hegazy AM, Abdelhiee EY. Anti-inflammatory, anti-oxidant and hepatoprotective effects of lactoferrin in rats. *Drug Chem. Toxicol*. 2021;44:286–293. doi: 10.1080/01480545.2019.1585868.

32- Tanaka H, Gunasekaran S, Saleh DM, Alexander WT, Alexander DB, Ohara H, et al. Effects of oral bovine lactoferrin on a mouse model of inflammation associated colon cancer. *Biochem. Cell Biol*. 2021;99:159–165. doi: 10.1139/bcb-2020-0087.

33- Venkatanarayana G, Sudhakara G, Rajeswaramma K, Indira P. Combined Effect of Curcumin and Vitamin E against CCl4 Induced Liver Injury in Rats. *American Journal of Life Sciences.* 2013; 1, (3):117-124. doi: 10.11648/j.ajls.20130103.17.

34- Naz S, Irshad F, Mawani, H. CCl4 Induced Liver Injury; Aqueous Extract of Ginkgo Biloba (Gkbe) Ameliorates

Cytoplasmic and Mitochondrial Enzymes. *The professional medical journal*.2017;*24*,739-744. doi: https://doi.org/10.29309/TPMJ/2017.24.05.1298.

35- Hassan N, Soliman G, Okasha E, Shalaby A. Histological, Immunohistochemical, and Biochemical Study of Experimentally Induced Fatty Liver in Adult Male Albino Rat and The Possible Protective Role of Pomegranate. *Journal of Microscopy and Ultrastructure*. 2018;6(1):44-55. doi: 10.4103/JMAU.JMAU_5_18. PMID: 30023266; PMCID: PMC6014250.

36- Abdeen M, Zaghloul D, Saleh R, Abdelmalek A. Histomorphometric Evidence of Hepatic Recovery of Rats Fed Repeatedly Heated Palm Oil. *Egyptian Journal of Histology*. 2022;45(1),115-124. doi: 10.21608/ejh.2021.57674.1415.

37- Kumar V, Abbas A, Aster J. *Robbin Basic Pathology. Chapter* (16) Liver and Gallbladder. 10th edition. Canada. Philadelphia. 2017.

38- Ogaly HA, Aldulmani SAA, Al-Zahrani FAM, Abd-Elsalam RM. D-Carvone Attenuates CCl_4-Induced Liver Fibrosis in Rats by Inhibiting Oxidative Stress and TGF-ß 1/SMAD3 Signaling Pathway. *Biology (Basel).* 2022;12;11(5):739. doi: 10.3390/biology11050739. PMID: 35625467; PMCID: PMC9138456.

39- Moreno MG, Chávez E, Aldaba-Muruato LR, Segovia J, Vergara P, Tsutsumi V, et al. Coffee prevents CCl(4)-induced liver cirrhosis in the rat. *Hepatol Int*. 2011;5(3):857-863. doi: 10.1007/s12072-010-9247-6. Epub 2011 Jan 25. PMID: 21484136.

40- Abd Elzaher F, Moussa M, Raafat M, Emara M. Histological Effect of Platelet Rich Plasma on CCL4 Induced Liver Fibrosis in Adult Albino Rat. *Egyptian Journal of Histology*. 2021;44(4),932-940. doi: 10.21608/ejh.2020.51054.1390.

41- Khedr NF, and Khedr EG. Antioxidant and Anti-inflammatory Effects of Curcumin on CCl4 – induced Liver Fibrosis in Rats. *Am. J. Biomed. Sci*. 2014, 6(3), 191-200. doi:10.5099/aj140300191.

42- Fujii T, Fuchs BC, Yamada S, Lauwers GY, Kulu Y, Goodwin JM, et al. Mouse model of carbon tetrachloride induced liver fibrosis: Histopathological changes and expression of CD133 and epidermal growth factor. *BMC Gastroenterol.* 2010;10:79. doi: 10.1186/1471-230X-10-79. PMID: 20618941; PMCID.

43- Lee Y, Cho I, Kim J, Lee M, Ku S, Choi J, et al. Hepatoprotective Effects of Blue Honeysuckle on CCl4-Induced Acute Liver Damaged Mice. *Food Science & Nutrition.* 2019;7(1):322–338. doi: 10.1002/fsn3.893.

44- Eldesouky NA, Elshopakey GE, Yusuf MS, Abdelhamid FM, Risha EF. Association between vitamin d deficiency and ccl4 mediated hepatic inflammation

in male albino rats; evaluation of some biochemical and antioxidant marker. *Adv. Anim. Vet. Sci*. 2021;9(7):994-1003. doi:10.17582/journal.aavs/2021/9.7.994.1003

45- Zowail M, Khater E, Waer H, Eltahawy N, Abd El-Hady A. Curative Effect of Bone Marrow Cells Transplantation and/or Low Dose Gamma Irradiation on Liver Injuries Induced by Carbon Tetrachloride. T*he Egyptian Journal of Hospital Medicine.* 2012;46: 96-114. doi: 10.21608/EJHM.2012.16362.

46- Amer MA, Othman AI, El-Missiry MA, Farag AA, Amer ME. Proanthocyanidins attenuated liver damage and suppressed fibrosis in CCl4-treated rats. *Environ Sci Pollut Res Int*. 2022;29(60):91127-91138. doi: 10.1007/s11356-022-22051-7. PMID: 35881285; PMCID: PMC9722827.

47- Fathy M, Okabe M, Saad Eldien H, Yoshida T. AT-MSCs Antifibrotic Activity Is Improved by Eugenol Through Modulation of TGF-B/Smad Signaling Pathway in Rats. *Molecules*. 2020;25(2):348-365. doi: 10.3390/molecules25020348.

48- Chen HA, Chiu CC, Huang CY, Chen LJ, Tsai CC, Hsu TC, et al. Lactoferrin Increases Antioxidant Activities and Ameliorates Hepatic Fibrosis in Lupus-Prone Mice Fed with a High-Cholesterol Diet. *J. Med. Food.* 2016;19:670–677. doi: 10.1089/jmf.2015.3634.